Extreme near-fault strong-motion of the M6.3 Ölfus earthquake of 29 May 2008 in South Iceland

B. Halldórsson, R. Sigbjörnsson & R. Rupakhety
University of Iceland, Earthquake Engineering Research Centre, Iceland

A.A. Chanerley
University of East London, United Kingdom

ABSTRACT
The M_w6.3 Ölfus earthquake of 29 May 2008 in Iceland occurred in the District of Ölfus in the western part of the South Iceland Seismic Zone. The earthquake rupture took place on two parallel and vertical right-lateral strike slip faults, separated by ~4 km, with the second fault rupturing shortly after the first. The town of Hveragerdi, being in the extreme near-fault region of the earthquake, suffered the heaviest damage. The strong motion in the town was recorded on 11 instruments of the ICEARRAY, a new small-aperture strong-motion array. These unique recordings all exhibit prominent long-period velocity pulses along both the strike-normal and strike-parallel horizontal directions. The linear response spectra indicate that the long-period energy of the velocity pulse seen along the strike-normal direction is not present in the strike-parallel direction. Furthermore, the period of the pulse is shorter along the strike-parallel and it is more narrow-banded in the elastic response spectrum than the pulse seen on the strike-normal component. The acceleration time histories have been baseline corrected using a new method and integrated to velocity and displacement. The corrections confirm that both the strike-normal and strike-parallel components are associated with considerable permanent tectonic displacement. The results of tectonic translation using this method agree with geodetic measurements near Hveragerdi, but the displacement estimates show some variability across the array. Finally, we show how the salient features of the near-fault ground displacement can be captured through kinematic modeling when adopting static slip distributions for the causative faults, and assuming uniform rise times and spreading rupture fronts. The results indicate that rupture on the second fault initiated ~2 s after the initial rupture on the first fault.

Keywords: ICEARRAY, earthquake, near-fault, strong-motion, translation

1. INTRODUCTION

Iceland is an island in the North Atlantic Ocean where the asthenosperic flow under the divergent plate boundary of the North American and the Eurasian plates interacts with a deep seated mantle plume, causing the dynamic uplift of the Iceland plateau with high volcanic productivity and thicker crust. On land the active volcanic zones generally follow the spreading axis of the plate margin (see gray line, bottom right in Figure 1). The rift axis in Iceland is offset via two transform fault zones, the Tjörnes Fracture Zone (TFZ) in the north and the South Iceland Seismic Zone (SISZ) in the south. The largest earthquakes in Iceland have taken place in these zones.

In contrast to the TFZ which is largely offshore, the SISZ is a populous agricultural region with numerous towns and villages, along with essential modern-day infrastructure and lifelines, such as pipelines, electric transmission systems, bridges, hydro-electric powerplants and dams. As a consequence, the seismic risk in the SISZ is relatively high. Strong earthquakes in the SISZ occur along near vertical north-south oriented dextral faults. The latest damaging earthquakes in the SISZ are the 17 June 2000 M_w6.5, the 21 June 2000 M_w6.4 (Sigbjörnsson & Ólafsson, 2004) and the 29 May 2008 M_w6.3 earthquakes, the last of which is the subject of this paper (Sigbjörnsson *et al.*, 2009).

The 29 May 2008 M_w6.3 Ölfus earthquakes ruptured the westernmost part of the SISZ, the densely populated Ölfus region between the towns of Hveragerdi and Selfoss (see Figure 1). The earthquake caused widespread damage in the area and was well recorded on the Icelandic Strong-motion Network (IceSMN; Sigbjörnsson *et al.*, 2004; Sigbjörnsson *et al.*, 2009) and the new Icelandic small-aperture strong-motion array (ICEARRAY) in the town of Hveragerdi (Halldorsson *et al.*, 2009; Halldórsson & Sigbjörnsson, 2009). In this paper we focus on the ICEARRAY small-aperture strong-motion array and its extreme near-fault recordings of the Ölfus earthquake. In particular, we discuss the baseline corrected velocity and displacement time histories, the observed permanent tectonic translation and compare with some results from kinematic modeling of the earthquake.

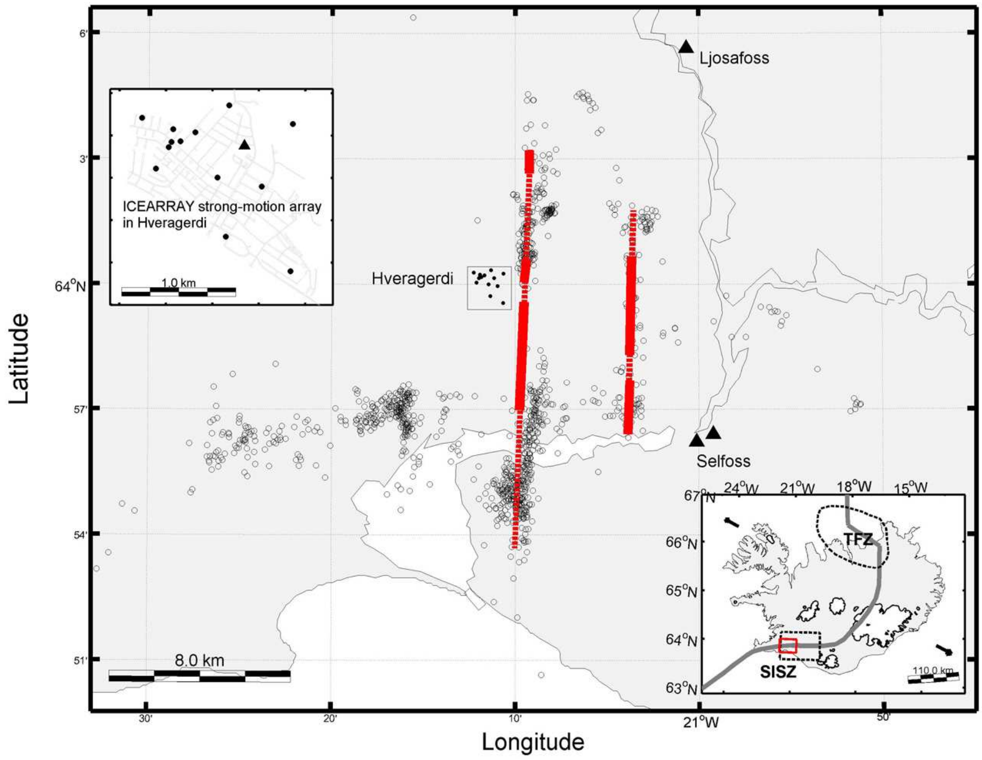

Figure 1. The small map inset at bottom right shows Iceland, an island in the North Atlantic Ocean, in reference to the present-day boundary (gray line) of the Eurasian and North American tectonic plates. Transform fault zones are indicated with dashed lines. The solid red rectangle within the SISZ indicates the macroseismic area of the Ölfus earthquake of 29 May 2008 (shown in the larger map) where the recording sites of the IceSMN are denoted as triangles and those of the ICEARRAY as dots (seen in the small map at top left along with the street layout of Hveragerdi). Aftershocks larger than M_L1.0 during 2 June to 10 July 2008 are shown in circles and the approximate locations of the causative faults by red dashed lines. The segments with largest slip according to Hreinsdottir *et al.* (2009) are indicated by a thicker solid red line.

2. THE M6.3 ÖLFUS EARTHQUAKE

At 15:45 UTC on 29 May 2008, a strong earthquake took place in the district of Ölfus, South Iceland, in the western part of the SISZ. The moment magnitude of the earthquake was 6.3 according to the CMT database and the INGV. The earthquake shares similar characteristics to other historical damaging earthquakes in the SISZ: shallow crustal earthquakes rupturing a near vertical north-south trending, right-lateral strike-slip fault (Sigbjörnsson *et al.* 2009). Over the first few days after the mainshock, the spatial distribution of aftershocks (from SIL network database, see e.g., Stefánsson *et al.* 1993; Halldorsson & Avery, 2009) suggested that a pair of faults ruptured during the earthquake, as indicated in Figure 1. The north-south trending distribution outlines an almost 10 km long north-south trending vertical fault near Selfoss (Ingolfsfjall fault). The main aftershock activity, however, shows an additional and nearly twenty km long alignment of aftershock epicentres indicating a north-south trending fault near the town of Hveragerdi (Kross fault) ~4 km west of the first one.

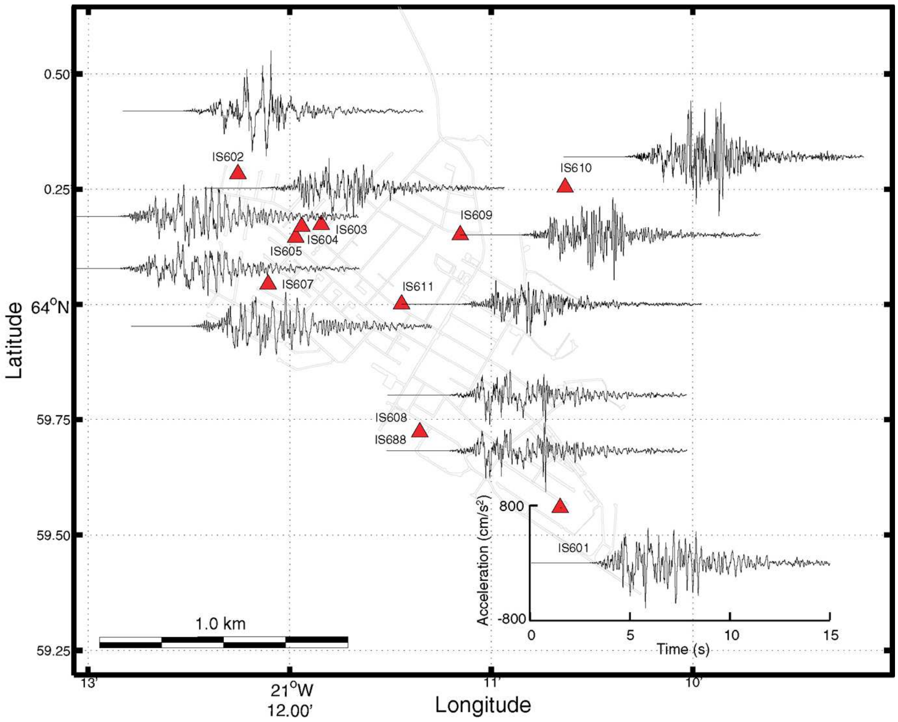

Figure 2. Segments of the north-south (SP) component of recorded acceleration time histories on the ICEARRAY stations during the Ölfus earthquake. The triangles denote the station locations (stations IS608/688 are collocated) and the gray lines show the street layout of Hveragerdi.

Geodetic measurements in the macroseismic area have shown that there was a significant and permanent tectonic offset in the near-fault region associated with the Ölfus earthquake. In general, the measurements indicate coseismic translation of Hveragerdi of ~19 cm northwest while Selfoss moved ~20 cm southeast (Hreinsdottir *et al.*, 2009; Decriem *et al.*, 2010). The geodetic studies using GPS measurements and satellite radar data (InSAR) of the macroseismic area show that the offset is best explained by a complex earthquake doublet where the slip took place on two parallel vertical right-lateral strike slip faults spaced ~4-5 km apart, where the first fault is estimated to have magnitude M_w5.8-6.1 and the second fault M_w5.9-6.0 (Hreinsdottir *et al.*, 2009; Decriem *et al.*, 2010). Both studies estimate, within the constraints of the data used in the respective studies, the static slip distribution function on both causative faults. Space limits a detailed discussion of their results in this study but it is pointed out that the pattern of slip distributions differ in the locations of the subevents of significant slip and the general distribution of slip, especially on the Ingolfsfjall fault. Both studies however agree on the location of the largest slip on the Kross fault, being associated with the apparent "gap" in the aftershock distribution seen in Figure 1. The studies find that the maximum slip is ~1.9-2.0 m on Ingolfsfjall fault and ~1.4-1.6 m on the Kross fault (Hreinsdottir *et al.*, 2009; Decriem *et al.*, 2010). The only temporal parameter estimated by the studies is based on the analysis of limited high-rate (1 Hz) CGPS data indicating that the slip on the second fault initiated within 3 s of the initial main shock (Hreinsdottir *et al.* 2009).

3. NEAR-FAULT STRONG-MOTION RECORDINGS

The Earthquake Engineering Research Centre (EERC) of the University of Iceland operates the IceSMN, the only accelerograph network in Iceland. The ICEARRAY, the first small-aperture strong-motion array in Iceland, was deployed in the SISZ in the fall of 2007 for the specific purpose of establishing quantitative estimates of spatial variability of strong-motions, and investigating earthquake rupture processes and source complexities of future significant earthquakes in the region. For further details on the ICEARRAY and its recordings of the Ölfus earthquake the reader is directed to the papers by Halldorsson and colleagues listed in the references.

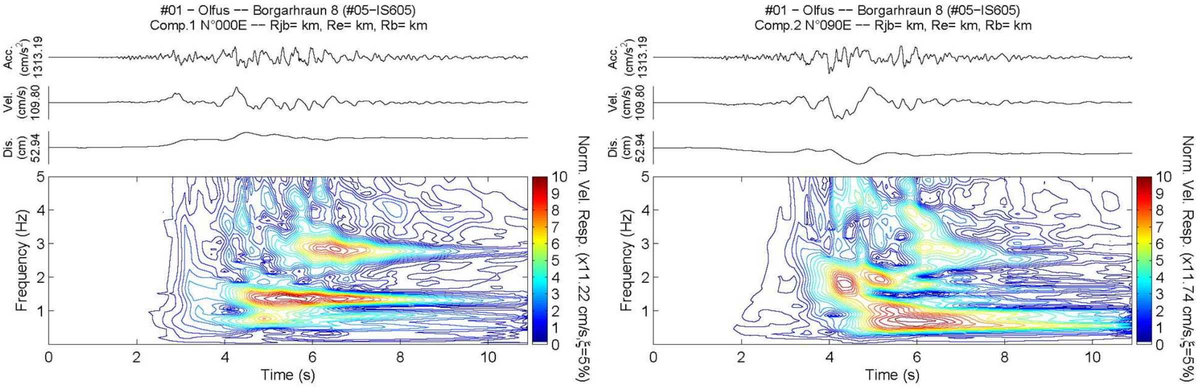

Figure 3. Velocity response envelope spectra of a linear elastic SDOF oscillator at station IS605 subjected to the SP (left) and SN (right) components of the acceleration recorded at the site. At the top the corresponding corrected acceleration, velocity and displacement time histories are shown.

During the earthquake the ICEARRAY produced high-quality three-component recordings at 11 stations in the extreme near-fault region, and the IceSMN recorded the earthquake at nine additional stations, three of which are in the near-fault region in the town of Selfoss. Figure 2 shows segments of the north-south (strike-parallel; SP) component of recorded acceleration time histories on the ICEARRAY stations during the Ölfus earthquake. The ICEARRAY recordings are characterized by strong motion of short duration of 4-5 s and high intensity, manifested by the horizontal PGA in Hveragerdi ranging between 38 and 88%g. There was evidence that the vertical acceleration had exceeded the acceleration of gravity in the near-fault region (g). The earthquake action on buildings in general exceeded the codified design loading with widespread and significant damage, even though the structural integrity of the majority of buildings was not compromised. This is believed to be due to the short duration of the strong motion and the natural strength of the relatively stiff low-rise buildings that are predominant in the area (Sigbjornsson *et al.* 2009; Halldorsson & Sigbjornsson, 2009).

It is well known that in the near-fault region of earthquake rupture in general, forward directivity effects of fault rupture and permanent tectonic translation effects are the two main causes of prominent and long-period velocity pulses observed along the strike-normal (SN) and strike-parallel (SP) directions, respectively, (e.g., Mavroeidis and Papageorgiou 2003, 2010). Indeed, the uncorrected velocity time histories calculated from the raw acceleration records reveal significant long-period velocity pulses on both SN and SP components (Halldorsson & Sigbjornsson, 2009).

Halldorsson and Sigbjornsson (2009) calculated the the corresponding linear pseudo-acceleration spectral response of a linear elastic SDOF oscillator with 5% damping ratio. They noted that the long-period energy evident on the SN component was not observed on the SP component, which exhibits a more narrow-band energy at 0.6–0.7 s period (~1.5 Hz). These different features become clearer when inspecting the velocity response envelope spectra seen in Figure 3. The SP component shows that the largest velocity response is primarily associated with oscillators of natural frequency centred at ~1.4 Hz. In turn, the SN component shows that the primary velocity response first occurs briefly at f~1.8 Hz and then shifts down to frequencies below 1.0 Hz. The temporal onset of this latter energy component occurs at around the same time as the one on the SP component. It appears therefore that forward directivity effects and translation effects act together on the SN component.

4. BASELINE CORRECTION PROCEDURE

The amount and direction of the tectonic translation measured near e.g. Hveragerdi implies that the corresponding acceleration should be evident on the recorded components. Therefore, we need to correct and integrate the acceleration recordings to reveal estimates of the “true” ground velocity and displacement as a function of time. Additionally, this will show in great detail the characteristics of the dynamic coseismic translation which cannot be provided by the geodetic measurements.

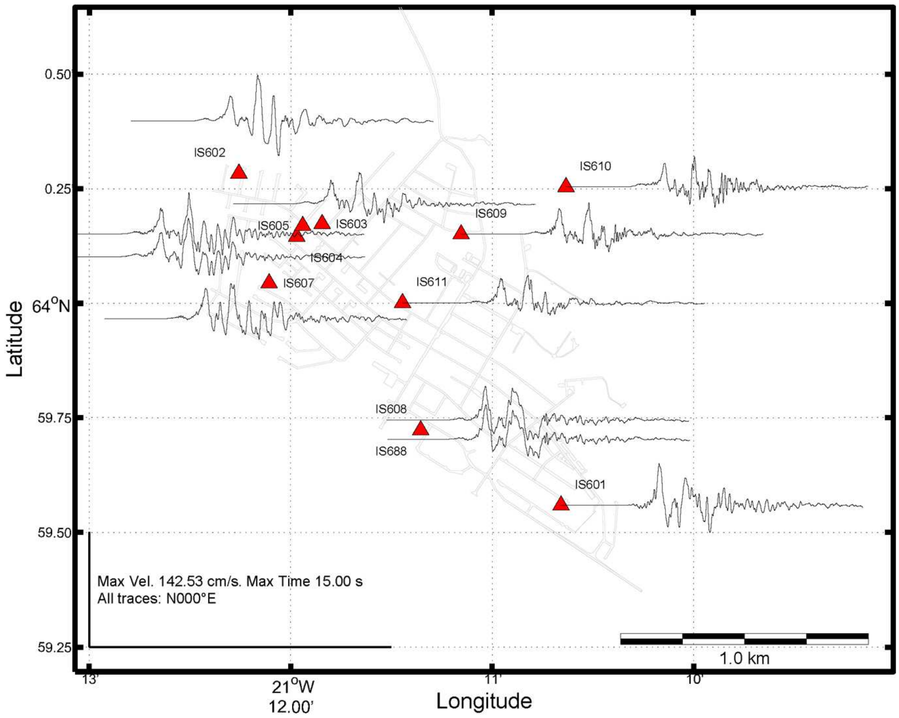

Figure 4. The corrected velocity time histories of the north-south (SP) component of recorded acceleration time histories in Figure 2. The amplitude and time bars on the left provide scale.

One of the problems associated with obtaining estimates of displacement is that standard filtering methods cannot extract the low frequency displacement from the acceleration time history. This is partly due to baseline shift brought about by integrating noise buried in the time history and partly by integrating distortions due to instrument tilts, cross-axis excitations and angular accelerations brought on by the seismic wave perturbing the ground. Usually the correction schemes try to locate time points at which to adjust for baseline shift evident after double time integration's of the acceleration time history recorded by the instruments.

In order to accurately estimate the velocity and displacement time histories from the ICEARRAY acceleration records, the latter need to be corrected for baseline shifts. This cannot be exactly done due to the instruments only recording the three translational components. However, a number of baseline correction methods exist in the literature that can be applied to this task (see e.g., Chanerley and Alexander, 2009; Rupakhety *et al.* 2009; and references therein).

In this study we apply the new baseline correction scheme of Rupakhety *et al.* (2009). Its primary assumption is that the ground displacement resembles a ramp step function between two time instants t_1 and t_3. Time t_1 can be set simply at the onset of the earthquake strong motion and t_3 is the earliest time the permanent offset has been attained. Their method applies an additional constraint on the latter time instant in that the low-frequency limit of the FAS of corrected velocity should be very close to the value of the final offset and that the FAS at low frequencies should be as flat as possible. They present a straightforward procedure for their baseline correction method and show that the results of their method are not sensitive to the selection of the model parameters or the strong-motion record analysed.

5. RESULTS

The values of the final displacement offset across the ICEARRAY during the 29 May 2008 earthquake have been estimated by Chanerley *et al.* (2009) and Rupakhety *et al.* (2009). The corrected velocity and displacement time histories on the basis of the wavelet correction method are presented in Halldorsson *et al.* (2010). Here however, we show the corrected velocity and displacement time histories according to the baseline correction procedure of Rupakhety *et al.* (2009). Figure 4 shows the SP component of corrected velocity time histories corresponding to the acceleration shown in Figure 2. The SP velocity time histories clearly show the presence of prominent long-period and large amplitude near-fault velocity pulses. It is also evident that there is variability in the velocity waveforms, while the long-period velocity pulses are common on all waveforms which can be approximated by two unipolar (positive) velocity pulses separated ~1.5 seconds apart.

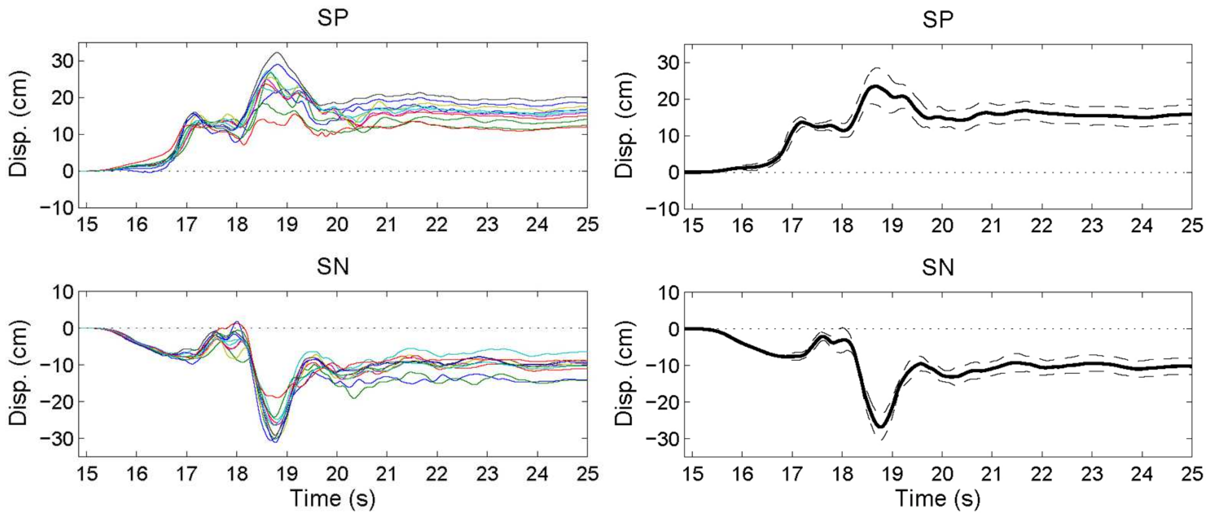

Figure 5. Left: The individual displacement time histories at ICEARRAY stations along the SP and SN directions at top and bottom, respectively, according to the correction method applied. Right: The mean displacement and its corresponding $\pm\sigma$. The time window starts at the arrival of the first P wave and the waveforms have been aligned at time instants giving maximum velocity waveform correlation.

The baseline corrected displacements along the SN (positive towards East) and SP (positive towards North) directions are shown for each individual station in Figure 5, along with the corresponding mean displacements and their corresponding $\pm\sigma$. It appears that that the displacement results for the SP component show greater variability than for the SN component.

The corrected displacement time histories reveal a mean tectonic translation of 15.96 ± 2.49 cm towards north, 11.24 ± 1.88 cm towards west, with a resultant mean horizontal translation of 19.63 ± 2.24 cm cm (Rupakhety *et al.*, 2009). This compares well with the published offset of 19.09 ± 0.09 cm resultant displacement near Hveragerdi, acording to GPS measurements (Hreinsdottir *et al.*, 2009).

It is evident that the strong-motion data from the Ölfus earthquake contains seismic waves radiating from two separate causative faults, arriving almost simultaneously. The strong-motion data indicates that the first motions originated on the Ingolfsfjall fault. To provide insight into the details of the recorded strong motion at Hveragerdi and Selfoss, respectively, we have simulated the low-frequency motions from each fault individually on the base of the static slip distributions of Hreinsdottir *et al.* (2009) assuming a circular sweeping rupture front and four discrete rise time values. The simulations were done using the discrete wavenumber method with point sources distributed over the fault planes. Through trial and error we have summed up the resulting motions with different combinations of rise times and time delay of the rupture of the Kross fault relative to the Ingolfsfjall fault. The results for the uniform rise times of 1.2 s and 0.5 s for the Ingolfsfjall and Kross faults respectively, with the rupture onset of the latter fault being 2.1 s after the initial break, are shown in Figure 6. The results from this simple approach are encouraging and appear to capture the primary features of the strong motion on all components at both stations. The main difference observed is that the simulated SN motion at Hveragerdi does not result in the considerable westward translation evident in the data. We are tempted to explain this discrepancy by the lack of counterclockwise block rotation that invariably occurs between parallel dextral faults, and is not taken into account in the simulations.

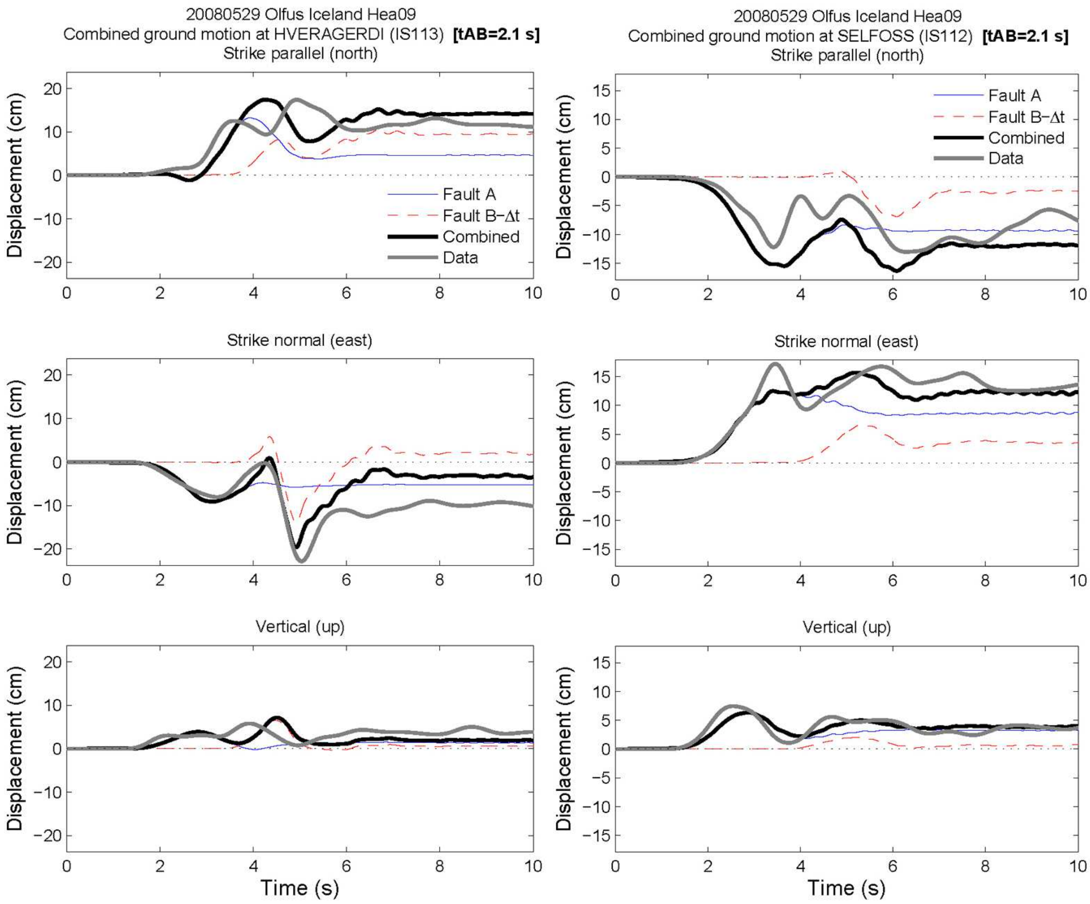

Figure 6. Comparison of the corrected displacement time histories (thick gray line) at station IS609 in Hveragerdi (left) and IS112 in Selfoss (right) with the corresponding synthetic motion from the kinematic simulations. The individual synthetic motions from the Ingolfsfjall fault (Fault A, solid blue) and the Kross fault (Fault B, dashed red) have been combined (thick black line) assuming a time delay of 2.1 seconds between their respective onsets of rupture.

6. CONCLUSIONS

We have estimated the corrected velocity and displacement time histories from the recorded acceleration in the near-fault region of the 29 May 2008 M_w6.3 Ölfus earthquake using the baseline correction method of Rupakhety *et al.* (2009). The displacement records show a permanent coseismic offset along both SP and SN directions in agreement with geodetic measurements. Across the ICEARRAY the velocity and displacement time histories have strong common features, respectively, but significant variability in particle motion is observed even over very short distances. The variability is most likely caused by local site effects and in few cases by non-uniform station setup conditions. Future work is focused on estimating this degree of variability and its causes, including comparing the baseline correction results of the two methods that have been used for that purpose on the ICEARRAY data. The purpose is to evaluate the “true” variability of ground motion across the ICEARRAY during the earthquake. Finally we show an example of how the main features of the three-component ground displacement time histories in the near-fault region can be adequately reproduced from given static slip distributions on the two faults through kinematic modeling of the earthquake. The results shown simply assume uniform sweeping rupture fronts and uniform rise times values over the respective causative faults, and a delay of 2.1 s between their onsets of rupture.

ACKNOWLEDGEMENTS

ICEARRAY is funded by the 6th Framework of the European Commission through the Marie Curie International Re-integration Grant (MC-IRG), contract No. MIRGCT-2006-036564, the Icelandic Centre for Research (RANNIS) Project Grants No. 60043021 and 90049022, the University of Iceland Research Fund, and the Síminn telecommunication company.

REFERENCES

Chanerley, A. A. and N. A. Alexander (2009). Obtaining estimates of the low-frequency 'fling', instrument tilts and displacement timeseries using wavelet decomposition, *Bulletin of Earthquake Engineering*. **8**:**2**, 231-255.

Chanerley, A. A., N. A. Alexander and B. Halldorsson (2009). On fling and baseline correction using quadrature mirror filters. *12th International Conference on Civil, Structural and Environmental Engineering Computing (CC2009)*, Funchal, Madeira, Portugal, 1-4 September 2009.

Decriem, J., Árnadóttir, T., Hooper, A., Geirsson, H., Sigmundsson, F., Keiding, M., Ófeigsson, B. G., Hreinsdóttir, S., Einarsson, P., LaFemina, P. & Bennett, R. A. (2010). The 2008 May 29 earthquake doublet in SW Iceland . *Geophysical Journal International*. **181:2**, 1128-1146.

Halldorsson, B. and H. Avery (2009). Converting strong-motion networks to arrays via common-triggering, *Seismological Research Letters*. **80:4**, 572-578.

Halldorsson, B. and R. Sigbjornsson (2009). The Mw6.3 Ölfus Earthquake at 15:45 UTC on May 29 2008 in South Iceland: ICEARRAY strong-motion recordings. Soil Dynamics and Earthquake Engineering. **29:6**, 1073-1083.

Halldorsson, B., R. Sigbjornsson and J. Schweitzer (2009). ICEARRAY: the first small-aperture, strong-motion array in Iceland. *Journal of Seismology*. **13:1**, 173–178.

Halldorsson, B., Sigbjörnsson, R., Chanerley, A. A. & Alexander, N. A. (2010). Near-fault strong-motion array recordings of the Mw6.3 Ölfus earthquake on 29 May 2008 in Iceland . *9th US National and 10th Canadian Conference on Earthquake Engineering (9USN/10CCEE)*, Paper no. 1157 (accepted).

Hreinsdóttir, S. Th. Árnadóttir, J. Decriem, H. Geirsson, A. Tryggvason, R. A. Bennett and P. LaFemina (2009). A complex earthquake sequence captured by the continuous GPS network in SW Iceland, *Geophysical Research Letters*, **36**, L12309.

Mavroeidis, G. P. & Papageorgiou, A. S. (2003). A Mathematical Representation of Near-Fault Ground Motions. *Bulletin of the Seismological Society of America*, **93:3**, 1099-1131.

Mavroeidis, G. P. and Papageorgiou, A. S. (2010). Effect of fault rupture characteristics on near-fault strong ground motions, *Bulletin of the Seismological Society of America*, **100:1**, 37-58.

Rupakhety, R., B. Halldorsson and R. Sigbjornsson (2009). Estimating coseismic deformations from near source strong motion records: Methods and case studies. *Bulletin of Earthquake Engineering* (published, online).

Sigbjörnsson, R. and Ólafsson, S. (2004). On the South Iceland Earthquakes in June 2000: Strong-Motion Effects and Damage. *Bollettino di Geofisika Teorica ed Applicata*, **45**, 131-152.

Sigbjörnsson, R., J.Th. Snæbjörnsson, S. M. Higgins, B. Halldórsson, S. Ólafsson (2009). A note on the M6.3 earthquake in Iceland on 29 May 2008 at 15:45 UTC. *Bulletin of Earthquake Engineering*, **7:1**, 113-126.

Sigbjörnsson, R., Ólafsson, S. and Thórarinsson, Ó. (2004). Strong-Motion Recordings in Iceland. *Proceedings of the 13th World Conference on Earthquake Engineering (13WCEE)*, Vancouver, BC, Canada, Mira, Paper No. 2370.

Stefánsson, R., R. Böðvarsson, R. Slunga, P. Einarsson, S. S. Jakobsdóttir, H. Bungum, S. Gregersen, J. Havskov, J. Hjelme, and H. Korhonen (1993). Earthquake Prediction Research in the South Iceland Seismic Zone and the SIL Project. *Bulletin of the Seismological Society of America*, **83**, 696-716.